Neurosurgical Review (2020) 43:473–482
https://doi.org/10.1007/s10143-018-1012-7

REVIEW

# Review of the main surgical and angiographic-oriented classifications of the course of the internal carotid artery through a novel interactive 3D model

Marc Valera Melé[1,2] · Anna Puigdellívol-Sánchez[1,3] · Marija Mavar-Haramija[1] · Juan A. Juanes-Méndez[4] · Luis San Román[5] · Matteo De Notaris[6] · Giuseppe Catapano[6] · Alberto Prats-Galino[1]

Received: 22 March 2018 / Revised: 31 May 2018 / Accepted: 10 July 2018 / Published online: 26 July 2018


## Abstract

The course of the internal carotid artery (ICA) and its segment classifications were reviewed by means of a new and freely available 3D interactive model of the artery and the skull base, based on human neuroimages, that can be freely downloaded at the Public Repository of the University of Barcelona (http://diposit.ub.edu/dspace/handle/2445/112442) and runs under Acrobat Reader in Mac and Windows computers and Windows 10 tablets. The 3D-PDF allows zoom, rotation, selective visualization of structures, and a predefined sequence view. Illustrative images of the different classifications were obtained. Fischer (Zentralbl Neurochir 3:300–313, 1938) described five segments in the opposite direction to the blood flow. Gibo-Rothon (J Neurosurg 55:560–574, 1981) follow the blood flow, incorporated the cervical and petrous portions, and divided the subarachnoid course—supraclinoid—in ophthalmic, communicating, and choroidal segments, enhancing transcranial microscopic approaches. Bouthillier (Neurosurgery 38:425–433, 1996) divided the petrous portion describing the lacerum segment (exposed in transfacial procedures and exploration of Meckel's cave) and added the clinoid segment between the proximal and distal dural rings, of interest in cavernous sinus surgery. The Kassam's group (2014), with an endoscopic endonasal perspective, introduces the "paraclival segment," including the "lacerum segment" and part of the intracavernous ICA, and details surgical landmarks to minimize the risk of injury. Other classifications are also analyzed. This review through an interactive 3D tool provides virtual views of the ICA and becomes an innovative perspective to the segment classifications and neuroanatomy of the ICA and surrounding structures.

**Keywords** Internal carotid artery segments · Anatomic models · Skull base anatomy · CT angiography · 3D angiography · 3D-PDF document

**Electronic supplementary material** The online version of this article (https://doi.org/10.1007/s10143-018-1012-7) contains supplementary material, which is available to authorized users.

✉ Anna Puigdellívol-Sánchez
apuigdellivol@ub.edu

[1] Laboratory of Surgical Neuroanatomy, Human Anatomy and Embryology Unit, Faculty of Medicine and Health Sciences, University of Barcelona, c/Casanova 143, 08036 Barcelona, Spain

[2] Hospital General Universitario Gregorio Marañón, Servicio de Neurocirugía, c/Dr Esquerdo 46, 28007 Madrid, Spain

[3] CAP Antón Borja, Consorci Sanitari de Terrassa, c/Edison s/n, 08191 Rubí, Spain

[4] VisualMed System Group, Human Anatomy and Histology Department, University of Salamanca, Av Alfonso X el Sabio s/n, 37007 Salamanca, Spain

[5] Clinic Center of Diagnostic by Imaging–Angioradiology, Hospital Clinic, c/Villarroel 170, 08036 Barcelona, Spain

[6] Neurosurgery Operative Unit, Department of Neuroscience, G Rummo Hospital, Via Pacevecchia 53, 82100 Benevento, Italy

## Introduction

The internal carotid artery (ICA) arises at the bifurcation of the common carotid artery (CCA) in the neck and extends to its final intracranial bifurcation into the middle cerebral artery (MCA) and the anterior cerebral artery (ACA). Several authors have proposed classifications of the course of the ICA with different number of segments (from 4 to 7), with some following or some not following the direction of the blood flow. According to Fischer's classification of 1938, the ICA was numbered in the opposite direction to blood flow [13]. The other authors followed the direction of the blood flow when describing four to seven segments, based on descriptions of the course of the ICA in cadaveric especimens, and extending from the cervical region [2, 15]. Most recently [23], in 2014, a new classification has been proposed based on a ventral endoscopic endonasal perspective.

Our group has previously shown that three-dimensional (3D) models enhance clinicians' anatomical and neurosurgical understanding of different regions of the skull base [5, 7], endonasal approaches to the ICA [4, 6, 8, 27], or structures involved in neuraxial anesthesia [32, 33]. Moreover, these 3D models may be embedded in interactive portable document format (PDF) files that may be opened in any freely available Adobe® Acrobat Reader® in desktop computers. Several 3D-PDF models based on human neuroimages, including the skull base, brain, optic chiasm, bilateral ICAs [4], or Vidian nerves and the possibility of selective bone structure removal (e.g., the middle turbinate) [27], were created to simulate extended endoscopic endonasal approaches and may be downloaded freely from the Electronic Supplementary material section [4] or from the Public Repository of the University of Barcelona at http://diposit.ub.edu/dspace/handle/2445/55224 [27], respectively.

We have now used that technology to assess the ICA anatomy, featuring its spatial disposition and main topographic relations, and have created a new interactive 3D-PDF [41].

The aim of this study is to review and compare four major classifications of ICA segments [2, 13, 23], through a new tool that improves the visualization of the complex 3D anatomy of the ICA and its relationships with adjacent structures.

## Material and methods

Illustrative images of the different classifications were obtained from a 3D-PDF interactive model of the ICA [41], which is freely available at the Public Repository of the University of Barcelona http://diposit.ub.edu/dspace/handle/2445/112442, and runs under Acrobat Reader in Mac and Windows computers and Windows 10 tablets. The study complied with the principles of the Declaration of Helsinki.

The development of a 3D-PDF [27, 33] from cranial CT angiography and 3D high resolution angiography images of a patient has been described previously [41]. Briefly, the process consisted in data acquisition, image processing (segmentation and surface reconstruction of bony and vascular structures), and the creation of a 3D PDF. The petrolingual ligament [PLL] was drawn at the level of the ICA as previously shown in cadaveric prossections [2, 23]. To illustrate the location of the dural rings, torus-3D-shaped structures were generated by 3D software (Amira 5.3, Mercury Co, Boston, USA) and located along the anterior loop of the ICA in accordance with previous ICA and dural ring descriptions and figures [2]. A template of the Gasserian ganglion (GG), from the visible ear [35] (0.3 mm of slice thickness) was generated and adapted to this model taking the petrous pyramid and skull foramens as references to position the ganglion. Finally, the 3D surface models of the ICA and of the neuroanatomical structures were exported together with the angio-TC 2D images as virtual reality model language (VRML) documents that may be embedded in 3D-PDF files.

The 3D-PDF allows zoom, rotation, selective visualization of structures, and a predefined sequence view. The 3D model includes the following structures: the skull base and the ICA with its main branches (ophthalmic artery [OphA], anterior choroidal artery [AChA], posterior communicating artery [PComA], middle cerebral artery [MCA], and anterior cerebral artery [ACA]) (Fig. 1), the GG, the PLL, and the proximal and distal dural rings (Fig. 2). The portions of the different segment classifications are colored in order to differentiate them. Four ICA models were created, one for each representative classification (Figs. 3, 4, 5, 6, and 7). A predefined coronal clipped view of the skull was generated to enhance the anatomic relations of the endoscopic perspective (Fig. 7).

## Results

### Review of the ICA course

The ICA was classically divided into "cervical," "petrous," and "cavernous" portions [45]. The successive segment classifications proposed additional parts within those portions (Table 1):

**Cervical portion** This is exocranial and has also been called "parapharyngeal" by some authors [23]. It extends from the junction with the common carotid artery at the C3–C4 or C4–C5 vertebral level to the entrance into the carotid canal within the petrous portion of the temporal bone.

**Petrous portion** The first "vertical" or "posterior ascending" portion within this canal [24], also named the "cochlear segment," [1] switches to a horizontal orientation after the so-called "posterior or genicular loop" [42], progressing anteromedially within the petrous pyramid (Fig. 1).

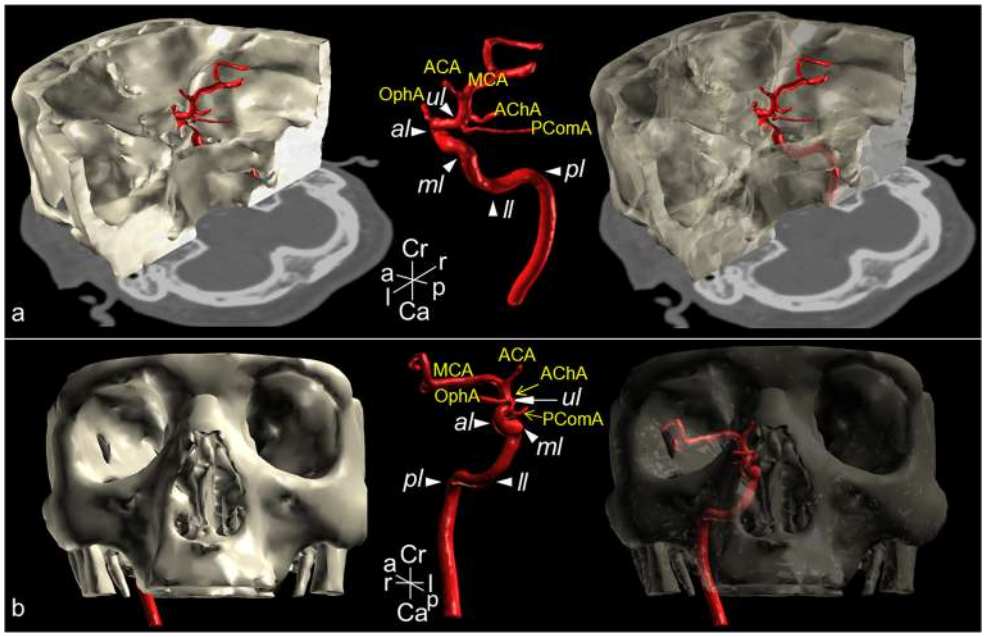


**Fig. 1** 3D-PDF images of the loops and branches of the ICA (center) from superolateral (**a**) or frontal endonasal (**b**) views. The 3D reproduced skull partially covers the course of the ICA (left images), but has been made partially transparent (right images) to allow visualization of the arterial course within the bone. The *loops* (*pl* posterior loop, *ll* lateral loop, *ml* medial loop, *al* anterior loop, *ul* unnamed loop) and branches of the ICA (*OphA* ophthalmic artery, *PComA* posterior communicating artery, *AChA* anterior choroid artery, *ACA* anterior cerebral artery, *MCA* middle cerebral artery) are labeled. Orientation: *Cr* cranial, *Ca* caudal, *a* anterior, *p* posterior, *l* left, *r* right

The ICA exits the bony canal but continues surrounded by periosteum, passing over the foramen lacerum, which is covered caudally by fibrocartilaginous tissue, the "ICA sock" [23]. Some authors define the "lacerum segment" at this level [2] (Fig. 6c) and consider this canalicular part to be the rostral extension of the carotid canal [38]. Another "loop" [2, 42] or "bend" [9] exists here, adjacent to the superomedial aspect of petrous apex, at the level of the superior edge of the petroclival

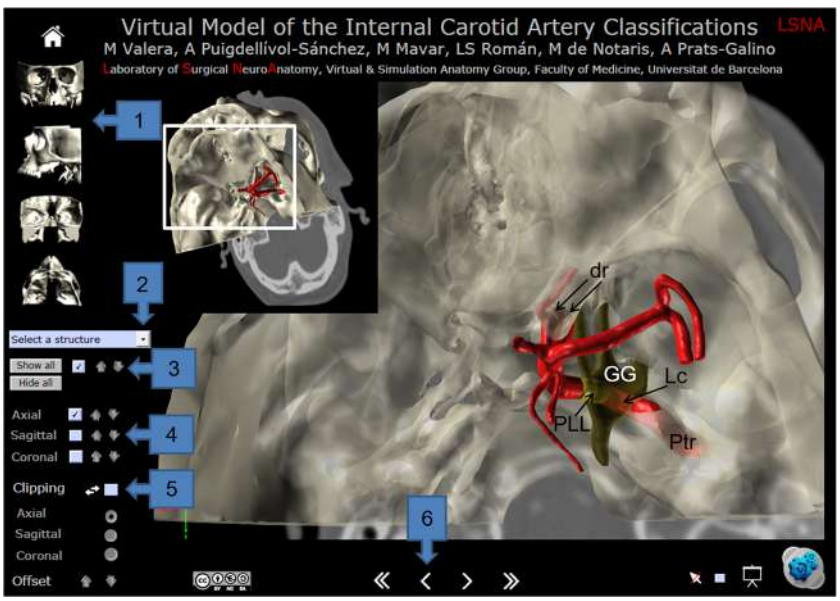


**Fig. 2** The 3D-PDF interface. A superolateral intracranial perspective is shown (enlarged rectangle area of the orientation picture at the top left zone). Either the skull and the Gasserian Ganglion (GG) have been partially transparented to enhance the visualization of the course of the ICA within the carotid canal of the petrous pyramid (Ptr), the lacerum portion (Lc) after which the ICA traverses the petrolingual ligament (PLL), entering at cavernous sinus. The inferior and superior dural rings (dr) are also visible under the anterior clinoid process. Commands: 1. Anterior, lateral, posterior, and superior sights. 2. Drop-down list of 3D reproduced structures. 3. Check box to show or hide specific 3D reproduced structures and arrows to increase or decrease transparency. 4. Selection and navigation among CT slices. 5. Clipping and navigation in the orthogonal planes. 6. Sequence of predefined views of the classifications of the ICA segments

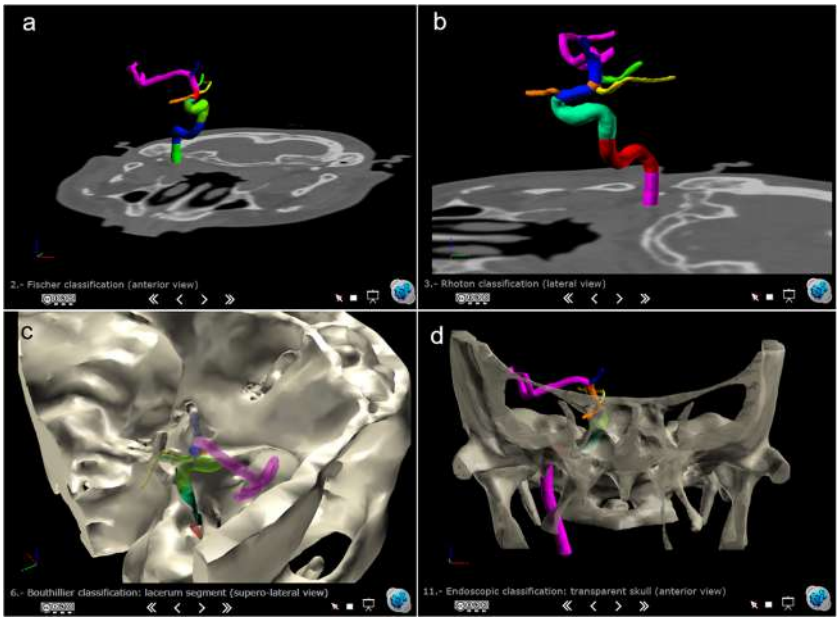


**Fig. 3** Predefined views of the different classifications. **a** Fischer's classification. **b** Rhoton's classification. **c** Bouthillier's classification. Superolateral view. Lacerum segment in dark green. **d** Anterior clipped view at the level of the sphenoidal sinus to show the course of the ICA from an endoscopic perspective. The skull has been made partially transparent

fissure [23], the so-called "lateral loop" [42] (Fig. 1), after which the ICA crosses the PLL. Distal to this ligament, the ICA enters the cavernous sinus [2] (Figs. 2, 3c, and 6a). Some authors have recently proposed the existence of the "precavernous ICA" [26], as a transitional segment between the "lacerum" and the "cavernous" segments.

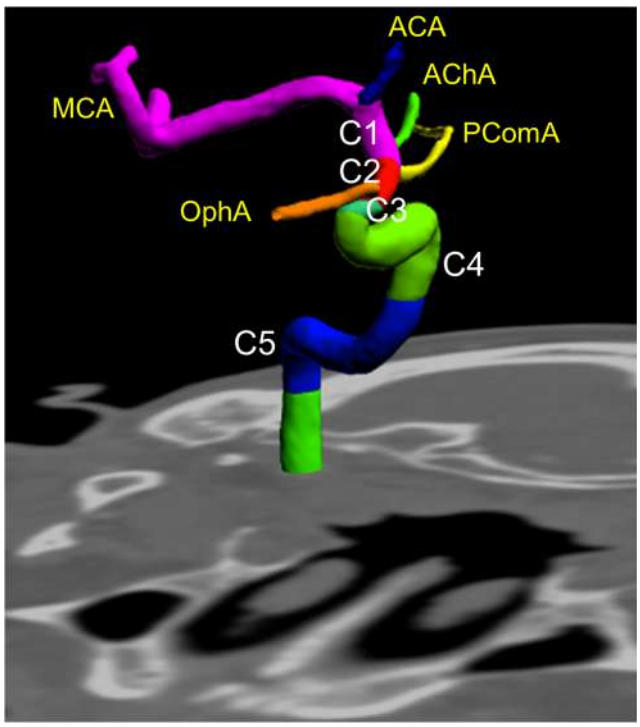


**Fig. 4** Fischer's classification. Detail of segments and main branches of the ICA. Anterior view. C5 segment (blue); C4 segment (green); C3 segment (dark green); C2 segment (red); C1 segment (purple). *OphA* ophthalmic artery, *PComA* posterior communicating artery, *AChA* anterior choroid artery, *ACA* anterior cerebral artery, *MCA* medial cerebral artery

**Cavernous portion** Within the cavernous sinus, the ICA continues rostrally in a medially ascending course. This part is considered by some authors as the "Gasserian" segment [1] since the GG is located just laterally outside the cavernous sinus (Fig. 6b) and "paraclival" by others [23]. At the level of the posterior clinoid process, a new loop (the so-called "medial" loop [42]) (Figs. 1a and 6b, c), after which the ICA continues horizontally beside the silla turcica ("parasellar" [23]) toward the "anterior" loop [42], between the proximal and distal dural rings, reaching the subarachnoid space at the level of the anterior clinoid process (Fig. 6c).

Some authors considered that the cavernous sinus ends when the ICA crosses the proximal dural ring [2, 23]. The portion between the proximal and distal dural rings is considered the "knee" of the ICA [13], the "clinoid" [2], the "paraclinoid" [23], or the "ring" segment [1]. The distal dural ring is the only complete ring that surrounds the ICA. This ring fuses laterally with the adventitia of the ICA and is continuous with the adjacent dura mater of the falciform ligament, the anterior clinoid process, and the roof of the cavernous sinus. The clinoid segment is part of the anterior loop of the ICA. The periosteum of the anterior clinoid and carotid sulcus covers much of this segment. The clinoid segment is covered by dura mater that is continuous with the roof of the cavernous sinus. If the anterior and middle clinoid processes fuse, the clinoid segment is surrounded by bone [2].

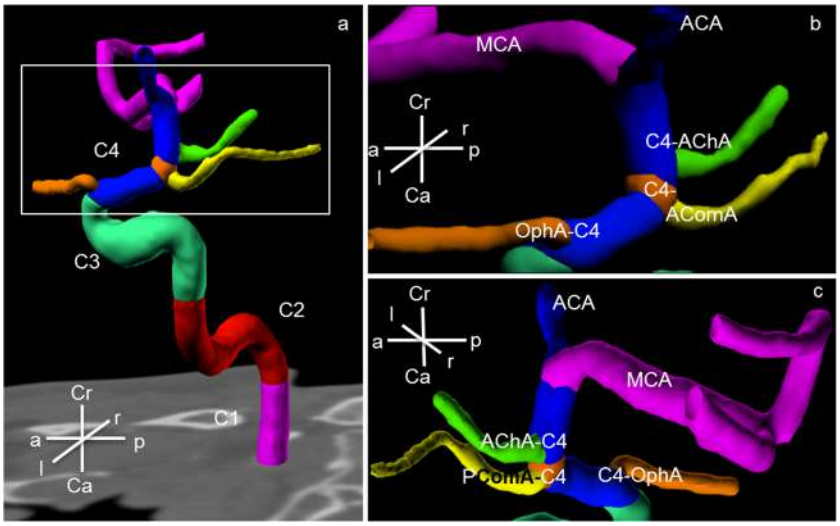


**Fig. 5** Rhoton's classification (medial view of the right ICA). **a** C1-cervical segment (purple); C2-petrous segment (red); C3-cavernous segment (dark green); C4-supraclinoid segment (ophthalmic segment in blue, communicating segment in orange, and choroidal segment in dark blue). **b** Detail of the rectangle in A. C4 or supraclinoid segment. Medial view, from the left side. **c** The same rectangle, lateral view, from the right side. *OphA* ophthalmic artery, *PComA* posterior communicating artery, *AChA* anterior choroid artery, *ACA* anterior cerebral artery, *MCA* middle cerebral artery, *Cr* cranial, *Ca* caudal, *a* anterior, *p* posterior, *l* left, *r* right

**The ICA at the subarachnoid space** After the ophthalmic artery origin, and usually immediately after the knee of the ICA [25], the artery progresses in a new anterior to posterior horizontal course that gives rise to the superior hypophyseal branches [25, 34]. This horizontal part ends in a final loop of the ICA (unnamed for the moment), initiating another ascending course that gives rise to the PComA and AchA before the bifurcation of the ICA into the ACA and MCA.

Some authors name this portion "cisternal" [1], "intradural" [23], or "supraclinoid" [15], defining subsegments ("ophthalmic" [2, 15], "communicating" [2, 15], "choroidal" [15]) (Fig. 5) at the level of the different branches of the ICA and being part of the carothid siphon [2, 15], inspired in the S shape of the ICA extending from the cavernous portion. The ophthalmic artery usually arises from the medial third of the superior surface of this portion, below the optic nerve, and medial to the anterior clinoid process. However, its origin may vary [25] by as much as 5 mm anterior to 7 mm posterior to the tip of the anterior clinoid process, and by between 2 and 10 mm medial to the clinoid process, but in some cases it has been found to emerge intradurally or as a branch of the inferolateral trunk of the cavernous segment. All those branches have been extensively described with accompagning illustrations and prosections [34].

## Review and comparison of segment classifications included in the 3D model

The comparison of the main ICA segment classifications is summarized in Table 1.

The Fischer's classification of 1938 was based on the angiographic appearance of its course (Figs. 3a and 4) [13]. The other classifications analyzed here are based on cadaveric dissections [2, 15, 23]. The classification proposed in 1981 by Gibo-Lenkey-Rothon [15] included a cervical segment (C1) and a petrous segment (C2) which ends where the artery enters the cavernous sinus (Figs. 3b and 5). They also considered that the cavernous segment (C3) terminated when the artery passed through the dura mater to form the roof of the cavernous sinus, at the entrance to the subarachnoid space. After this cavernous segment (C3), this classification divides the subarachnoid part of the ICA (here called supraclinoid or C4) in three subsegments (ophthalmic, communicating, and choroidal) related to the emergence of those arteries (Fig. 5b, c). The classification published in 1996 by Bouthillier [2] (Figs. 3c and 6) divided the previous petrous portion in "petrous" (C2) and "lacerum" portion (C3), which "begins where the carotid canal ends, which is at a vertical line at the posterolateral margin of the exocranial foramen lacerum," with ICA passing "above but not through" the lacerum foramen (Fig. 6c), before its entrance in the cavernous sinus. Bouthillier et al. [2] considered that the cavernous sinus ends at the level of the proximal dural ring and describes there a new "clinoid" segment, between the proximal and distal dural rings. The wide experience of the Kassam's group in the endoscopic surgery [19, 20] lead to the last classification reproduced in the 3D model that was recently published (2014) [23] and introduced a comprehensive scheme for the ICA, illustrated with extensive cadaveric prossections, from an endoscopic endonasal skull base perspective (Figs. 3d and 7) and detailed surgical landmarks for the distal anatomic border of each segment (Table 1, last column), working corridors, and modular approaches. The lacerum segment of the Bouthillier's classification is here included in the "paraclival" segment, that extends within the cavernous sinus until the

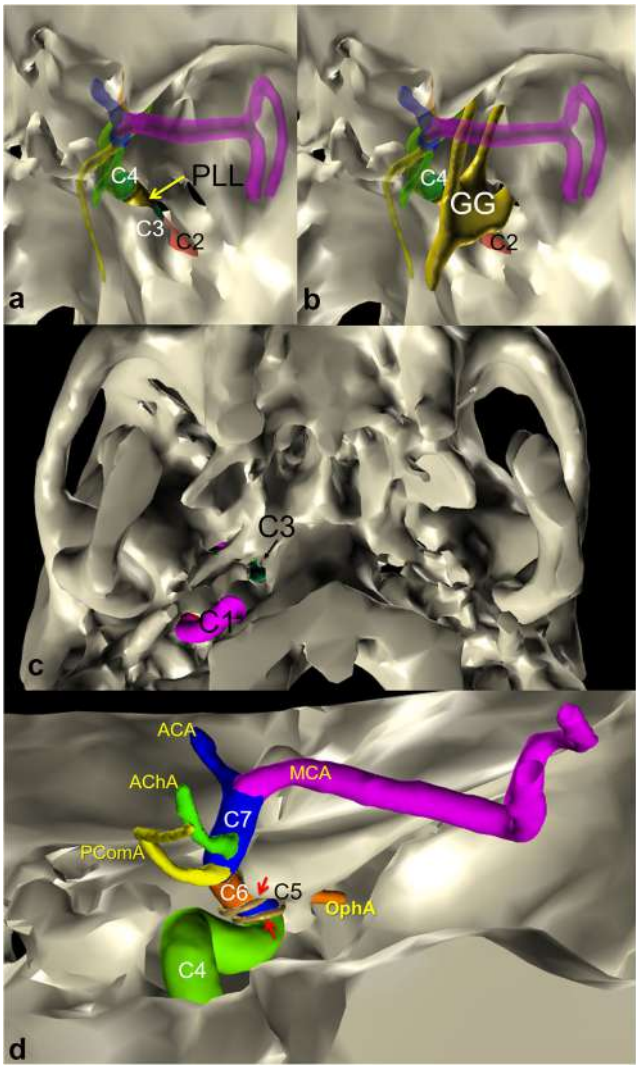


**Fig. 6** Bouthillier's classification. **a** Superolateral view. Petrolingual ligament (PLL) from the sphenoidal lingula to the petrous portion of the temporal bone, covering the lacerum segment (C3); C2-petrous segment (transparent red); C4-cavernous segment (transparent green). **b** Same perspective than image (**a**). Gasserian ganglion (GG) above the petrolingual ligament and covering the lacerum segment. **c** Foramen lacerum from an exocranial view, where the lacerum segment is seen in dark green (C3, arrow). C1-cervical segment (magenta) is also seen before getting inside the skull. **d** Posterior view. Proximal and distal dural rings (red circle), surrounding the clinoid segment of this classification. C4-cavernous segment (green); C5-clinoid segment (blue); C6-ophthalmic segment (orange); C7-communicating segment (dark blue). *OphA* ophthalmic artery, *PComA* posterior communicating artery, *AChA* anterior choroid artery, *ACA* anterior cerebral artery, *MCA* middle cerebral artery

level of superior edge of the petroclival fissure. Distally, the "parasellar" segment is also described within the cavernous sinus, limited by the proximal dural ring, followed by the "paraclinoid" segment (similar to the Bouthillier's "clinoid" segment (Table 1). Kassam coincides with Bouthillier when considering that this "paraclinoid" segment, between the proximal and distal dural rings, is outside the cavernous sinus.

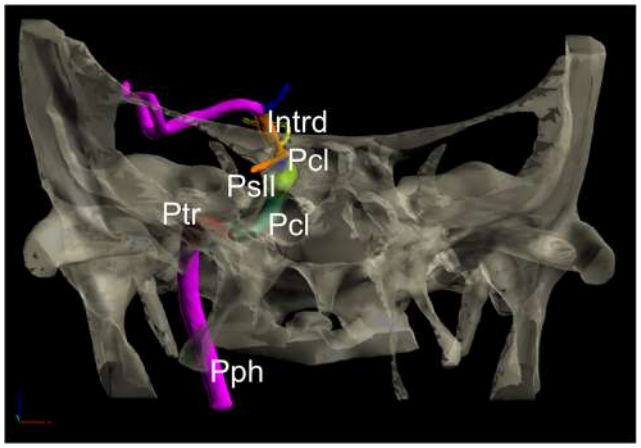


**Fig. 7** Endoscopic classification: transparent skull (anterior view). *Pph* parapharyngeal segment (purple), *Ptr* petrous segment (red), *Pcl* paraclival segment (dark green), *Psll* parasellar segment (green), *Pcl* paraclinoid segment (blue), *Intrd* intradural segment (orange)

The Labib-Kassam's "intradural" segment [23] would correspond to the full C4-"supraclinoid" segments of the Gibo-Lenkey-Rothon classification [15].

Some authors have tried to find a common nomenclature for the intracranial and endonasal approaches [9, 26]. Furthermore, the existence of a paratrigeminal "precavernous segment," a transitional segment between the C3 and C4 Bouthillier's classification, has been proposed. The medial aspect of such "precavernous" ICA would correspond with the "paraclival" ICA [26].

Altogether, an universally accepted classification providing a common nomenclature that enables communication between different disciplines, such as neurosurgery and neuroradiology, remains elusive.

## Clinical implications

One of the main goals of 3-D reconstructions of the course of the internal carotid artery is to understand how the different perspectives and the relative positions of the major supply route of blood to the brain may contribute to enhancing endovascular or surgical strategies. This understanding has the potential to improve our spatial interpretations: it opens up new possibilities in the decision-making process and in the choice of treatments, and may thus change our daily medical practice. Indeed, ICA is commonly affected by different and complex vascular and tumoral lesions.

Rupture of the extracranial carotid artery is a rare but potentially dramatic event, although covered stent grafting may solve it [3]. Cervical ICA can also be affected by parapharyngeal space tumors. Either an endoscopic-assisted transoral approach or transnasal transpterygoid approach may be used to expose these segments [37]. The parapharyngeal (or "cervical") ICA can be identified endoscopically posterolateral to the deepest aspect of the fossa of Rosenmüller [14, 23]. In case of

**Table 1** Classification of segments, including loops, branches, anatomical landmarks, and compartments of the ICA

| Anatomical compartments<br>Limits | ICA Loops<br>-Portions<br>main branches | Fisher<br>Angiographic<br>(1938) | Gibo-Lenkey-Rhoton Anatomical<br>(1981) | | Bouthillier<br>Anatomical<br>(1996) | | Kassam<br>Endoscopic<br>(2014) Surgical landmarks |
|---|---|---|---|---|---|---|---|
| Neck | CCA bifurcation | | C1 | Cervical | C1 | Cervical | Parapharyngeal |
| | (C3-C4 or C4-C5 vertebral level) | | | | | | Eustachian tube |
| | -Vertical or ascending portion | | | | | | Fossa of Rossenmüller |
| External orifice of carotid canal | | | | | | | Levator veli palatini muscle |
| Petrous piramid | Posterior loop | | C2 | Petrous | C2 | Petrous | Petrous |
| (temporal bone) | Caroticotympanic A | | | | | | Vidian canal, Pterygoid wedge |
| | -Horizontal portion | | | | | | |
| Foramen lacerum (posterolateral edge from an exocranial view) | (lateral to medial, posterior to anterior) | C5 | | | C3<br>ICA over the foramen (not through) | Lacerum | Fibrocartilague of foramen lacerum<br>Paraclival |
| | Lateral loop | | | | | | |
| PLL (superior aspect) | -Vertical or ascending portion | | | | | | |
| Cavernous sinus, beside GG | Inferolateral trunk | | C3 | Cavernous | C4 | Cavernous | |
| | Capsular branches | | | | | | |
| | Meningohypophyseal trunk | | | | | | Paraclival protuberance |
| Petrous apex (superomedial)≈ | | | | | | | Roof of fossa of Rossenmüller |
| petroclival fissure (superior edge) | | | | | | | ICA sock, foramen rotundum |
| | Medial loop | C4 | | | | | Parasellar |
| | -Horizontal portion | | | | | | |
| | (posterior to anterior) | | | | | | Sellar floor |
| Proximal dural ring | | C3 | | | C5 | Clinoid | Paraclinoid |
| Anterior clinoid process | Anterior loop | Knee of the ICA | | | | | Lateral tubercular recesses |
| Distal dural ring | | | | | | | Medial opticocarotid recesses |
| | | | | | | | Distal osseus arch |
| Subarachnoid space | Oph A | C2 | C4 | Ophthalmic | C6 | Ophthalmic | Intradural |
| | -Horizontal course | | | | | | |
| Optic nerve | (anterior to posterior) | | | | | | |
| | Superior hypophyseal A | | | | | | |
| | Loop (unnamed) PComA | C1 | | Communicating | C7 | Communicating | |
| | -Vertical course | | | | | | |
| | AChA | | | Choroidal | | | |
| | ICA bifurcation | | | | | | Cranial nerves II and III |

retropharyngeal displacements or infiltration by tumors, transoral robotic surgery has also provided promising results [17]. The transcervical approach is used in many cases of craniocervical paragangliomas of glomus jugulare, glomus tympanicum, and carotid body tumors in which the study of the ICA's anatomy is crucial to achieve a complete, incident-free tumor resection [31].

The petrous carotid artery must be exposed in four situations: aneurysms, tumors, atherosclerosis, and traumatic injuries. Revascularization techniques [40] have been described for treating aneurysms in the cervical and petrous segments of the ICA. Bypass techniques from cervical to petrous segments and also from middle meningeal artery to petrous segment have been studied for the management of high cervical vascular lesions and infratemporal fossa tumors invading the ICA. A thorough knowledge of the anatomy of the petrous segment of the ICA and its bony relationships could be helpful in many skull base approaches, such as the Kawase middle approach [21], when treating vascular lesions of the ICA or malignant tumors invading the skull base. Knowledge of the location of the Eustachian tube in relation to the petrous segment of the ICA is crucial when drilling the Glasscock triangle [16], in order to avoid cerebrospinal fluid rhinorrhea. The main risk of performing surgery in the nasopharynx is the potentially mortal rupture of the parapharyngeal or petrous ICA [14]. The petrous segment [39] and the angulation of its bends is variable [42, 43] and may receive collateral blood flow from the external carotid artery during ICA occlusion [22]. Twenty-five percent of cases may show a dehiscent bony roof of the horizontal petrous carotid canal that may facilitate exposure of the vessel in high-flow bypass procedures, with complete graft intracranial protection, avoiding the need for surgical neck exposure [36].

The lacerum segment has gained greater clinical significance because it is frequently exposed in surgical procedures, such as those involving both endoscopic endonasal and transfacial approaches exposing Meckel's cave [2, 38]. The recent definition of the "precavernous ICA" suggests a "safe door" for lesions in Meckel's cave, cavernous sinus, and petrous apex [26].

Nevertheless, through the endoscopic perspective, either the lacerum segment or the first part of the intracavernous ICA are considered together in the "paraclival" ICA. A fifth "posteroinferior" venous compartment within the cavernous sinus is described from that perspective, which can be enlarged by tumors, in addition to the "lateral," "medial," "anterior inferior," and "posterior superior" compartments [18], which are divided by the "parasellar" segment of the ICA [23]. Injuries to the ICA cause significant morbidity and mortality during endoscopic procedures reported to range from 0 to 3.8% [12]. Furthermore, the ICA is one of the vascular structures that is most exposed during skull base surgery. The endoscopic ventral perspective of the skull base and the identification of the different ICA segments is often difficult depending on the degree of pneumatization of the sphenoid sinus and the bulging and dehiscence of the ICA itself. Indeed, as previously stated, the classifications of the transcranial vision of the ICA do not necessarily corresponds to the ventral endoscopic endonasal view. Therefore, Kassam's classification represents a noteworthy effort to clarify the relationships of the ICA as seen from the ventral route. This classification describes the "parapharyngeal" and "paraclival" portions of the ICA thus obtaining a better understanding of these specific anatomical segments which present notable differences when compared with the intracranial view [23].

The supraclinoid portion is a common site of intracranial aneurysms [34] and its branches are frequently stretched or displaced by intracranial tumors [15]. The most common intracranial ICA aneurysms (accounting for approximately 35%) occur at four sites: the upper surface at the origin of the ophthalmic artery, the posterior wall at the origin of PComA, the posterior wall at the origin of the AChA, and at the apex of the bifurcation [15]. Among these localizations, the "knee" of the ICA, already recognized angiographically by Fischer [13], was definitively described when cavernous sinus surgery was developed [29] and this is a critical segment for the exposure of aneurysms of the ophthalmic segment. The supraclinoid portion is also exposed during most operations on tumors of the sphenoid ridge, anterior and middle cranial fossae, and sellar regions but these branches are only rarely sacrificed in removing the tumors. The different ways of exposing each of the supraclinoid branches, removing the anterior clinoid process and incising the falciform process to facilitate the exposure of the ophthalmic artery, the inspection of the PCoA through the triangular space between the optic nerve, the ICA and ACA, or opening the medial part of the Sylvian fissure below the anterior perforated substance to expose the choroidal segment, have extensively been described [15].

## 3D reconstructions and 3D-PDF models

Currently, there are sophisticated software applications that make possible to visualize, manipulate, and post-process medical images. Some of those tools are Free Open Source Code such as OsiriX (www.osirix-viewer.com) or 3D Slicer (www.slicer.org). The radiological equipments use also to include specific 3D software such as VITREA2 (Toshiba medical systems, Ōtawara, Japan) and AW VolumeShare 5 (General Electric, Fairfield, USA) that allow individualized 3D reconstructions [28]. These tools may allow to simulate a specific environment previously to a concrete surgery. Some experiences in pre-operative 3D reconstruction from RM or CT have recently been described [10, 11, 44].

Furthermore, the 3-D models obtained from cross-sectional images can be embedded in PDF files, making them a

powerful tool for clinical, educational, and research purposes [30]. The 3D-PDF files run under Acrobat Reader (XI or superior) in desktop computers and Windows 10 tablets but not in other tablets, smartphones, or Lynux systems, for the moment. Based on this extensive experience, we are confident that our interactive 3D-PDF prototypes of the ICA classifications provide a significant opportunity to improve the comprehension of the neuroanatomical relations of the artery and related vascular diseases, especially in the field of neurosurgery and neuroradiology.

## Conclusion

The present study provides the comparison of several major classifications of the ICA segments with the aid of an interactive and universally available 3D-PDF tool based on high-resolution angiography data to provide a new and deep approach to the knowledge of the neuroanatomy of the ICA and surrounding structures.

**Acknowledgements** The authors are grateful to Olga Fuentes for her contribution to image processing.

**Funding** This study was funded by the Fundació Marató TV3 Project [411/U/2011—TITLE: Quantitative analysis and computer aided simulation of minimally invasive approaches for intracranial vascular lesions].

### Compliance with ethical standards

**Conflict of interest** The authors declare that they have no conflict of interest.

**Ethical statement** All procedures were in accordance with the ethical standards of the institution and with the 1964 Helsinki declaration and its later amendments or comparable ethical standards.

## References

1. Abdulrauf SI, Ashour AM, Marvin E, Coppens J, Kang B, Hsieh TY, Nery B, Penanes JR, Alsahlawi AK, Moore S, Abou Al-Shaar H, Kemp J, Chawla K, Sujijantarat N, Najeeb A, Parkar N, Shetty V, Vafaie T, Antisdel J, Mikulec TA, Edgell R, Lebovitz J, Pierson M, Pires de Aguiar PH, Buchanan P, Di Cosola A, Stevens G (2016) Proposed clinical internal carotid artery classification system. J Craniovertebr Junction Spine 7:161–170 Erratum in J Craniovertebr Junction Spine (2016) 8:84
2. Bouthillier A, van Loveren HR, Keller JT (1996) Segments of the internal carotid artery: a new classification. Neurosurgery 38:425–433
3. Choi HC, Park SE, Choi DS, Shin HS, Kim JE, Choi HY, Park MJ, Koh EH (2018) Ruptured extracranial carotid artery: endovascular treatment with covered stent graft. J Neuroradiol 45:217–223
4. D'Avella E, De Notaris M, Enseñat J, Berenguer J, Gragnaniello C, Mavar M, Ferrer E, Prats-Galino A (2015) The extended endoscopic endonasal transplanum transtuberculum approach to the anterior communicating artery complex: anatomical study. Acta Neurochir 157:1495–1503
5. De Notaris M, Prats-Galino A, Cavallo LM, Esposito F, Iaconetta G, González JB, Montagnani S, Ferrer E, Cappabianca P (2010) Preliminary experience with a new three-dimensional computer-based model for the study and the analysis of skull base approaches. Childs Nerv Syst 26:621–626
6. De Notaris M, Solari D, Cavallo LM, Enseñat J, Alobid I, Soria G, Gonzalez JB, Ferrer E, Prats-Galino A (2011) The use of a three-dimensional novel computer-based model for analysis of the endonasal endoscopic approach to the midline skull base. World Neurosurg 75:106–113
7. De Notaris M, Palma K, Serra L, Enseñat J, Alobid I, Poblete J, González JB, Solari D, Ferrer E, Prats-Galino A (2014) A three-dimensional computer-based perspective of the skull base. World Neurosurg 82:S41–S48
8. De Notaris M, Prats-Galino A, Enseñat J, Topczewski T, Ferrer E, Cavallo LM, Cappabianca P, Solari D (2014) Quantitative analysis of progressive removal of nasal structures during endoscopic suprasellar approach. Laryngoscope 124:2231–2237
9. De Powell JJ, Froelich SC, Zimmer LA, Leach JL, Karkas A, Theodosopoulos PV, Keller JT (2014) Segments of the internal carotid artery during endoscopic transnasal and open cranial approaches: can a uniform nomenclature apply to both? World Neurosurg 82(6S):S66–S71
10. Dolati P, Golby A, Eichberg D, Abolfotoh M, Dunn IF, Mukundan S, Hulou MM, Al-Mefty O (2015) Pre-operative image-based segmentation of the cranial nerves and blood vessels in microvascular decompression: can we prevent unnecessary explorations? Clin Neurol Neurosurg 139:159–165
11. Dolati P, Eichberg D, Golby A, Zamani A, Laws E (2016) Multimodal navigation in endoscopic transsphenoidal resection of pituitary tumors using image-based vascular and cranial nerve segmentation: a prospective validation study. World Neurosurg 95: 406–413
12. Dusick JR, Esposito F, Malkasian D, Kelly DF (2007) Avoidance of carotid artery injuries in transsphenoidal surgery with the Doppler probe and micro-hook blades. Neurosurgery 60:322–328
13. Fischer E (1938) Die lageabweichungen der vorderen hirnarterie im gefäbild. Zentralbl Neurochir 3:300–313
14. Gao Z, Chi FI (2015) Anatomy relationship around internal carotid artery in the endoscopic surgery of nasopharynx: a study based on computed tomography angiography. J Neurol Surg B Skull Base 76:176–182
15. Gibo H, Lenkey C, Rhoton A Jr (1981) Microsurgical anatomy of the supraclinoid portion of the internal carotid artery. J Neurosurg 55:560–574
16. Glasscock ME III (1969) Middle fossa approach to the temporal bone. An otologic frontier. Arch Otolaryngol 90:15–27
17. Gorpe P, Auperin A, Honart JF, Ton Van J, El Bedoui S, Bidault F, Temam S, Kolb R, Qassemyar Q (2018) Revisiting vascular contraindicatios for transoral robotic surgery for oropharyngeal cancer. Laryngoscope Investig Otolaryngol 3:121–126
18. Harris FS, Rhoton AL (1976) Anatomy of the cavernous sinus. A microsurgical study. J Neurosurg 42:169–180
19. Kassam AB, Gardner P, Snyderman C, Mintz A, Carrau R (2005) Expanded endonasal approach: fully endoscopic, completely transnasal approach to the middle third of the clivus, petrous bone, middle cranial fossa and infratemporal fossa. Neurosurg Focus 19: E6
20. Kassam AB, Vescan AD, Carrau RL, Prevedello DM, Gardner P, Mintz AH (2008) Expanded endonasal approach: vidian canal as a landmark to the petrous internal carotid artery. J Neurosurg 108: 177–183
21. Kawase T, Shiobara R, Toya S (1991) Anterior transpetrosaltranstentorial approach for sphenopetroclival meningiomas: surgical method and results in 10 patients. Neurosurgery 28(6):869–875 discussion 875–876

22. Kim B (2010) Anatomy. Blood supply to the brain. In: Citow JS, Macdonald RL, Refai D (eds) Comprehensive neurosurgery board review, 2nd edn. Thieme, New York, pp 1–110
23. Labib M, Prevedello D, Carrau R, Kerr E, Naudy C, Abou Al-Shaar H, Corsten M, Kassam A (2014) A road map to the internal carotid artery in expanded endoscopic endonasal approaches to the ventral cranial base. Neurosurgery 10:448–471
24. Lasjaunias P, Berenstein A (1978) Arterial anatomy: introduction. In: Lasjaunias P, Berenstein A (eds) Surgical Neuroangiography: functional anatomy of craniofacial arteries. Springer-Verlag, Berlin, pp 1–32
25. Louw L (2015) Different ophthalmic artery origins: embriology and clinical significance. Clin Anat 28:276–576
26. Marcati E, Andaluz N, Froelich SC, Zimmer LA, Leach JL, Fernández-Miranda JC, Kurbanov A, Keller JT (2017) Paratrigeminal, paraclival, precavernous, or all of the above? A circumferential anatomical study of the C3-C4 transitional segment of the internal carotid artery. Oper Neurosurg (Hagerstown). https://doi.org/10.1093/on/opx121
27. Mavar-Haramija M, Prats-Galino A, Juanes-Méndez JA, Puigdellívol-Sánchez A, de Notaris M (2015) Interactive 3D-PDF presentations for the simulation and quantification of extended endoscopic endonasal surgical approaches. J Med Sys 39:127
28. Mujika KM, Méndez JAJ, de Miguel AF (2018) Advantages and disavantages in image processing with free software in radiology. J Med Sys 42:36
29. Nathal E, Castillo G (2012) Surgical treatment of paraclinoid aneurysms. In: Quiñones-Hinojosa A (ed) Schmidek and sweet operative neurosurgical techniques: indications, methods and results, 6th edn. Elsevier, Philadelphia, pp 855–871
30. Phelps A, Naeger DM, Marcovici P (2012) Embedding 3D radiology models in portable document format. AJR Am J Roentgenol 199:1342–1344
31. Prasad SC, Thada N, Pallavi, Prasad KC (2011) Paragangliomas of the head&neck: the KMC experience. Indian J Otolaryngol Head Neck Surg 63:62–73
32. Prats-Galino A, Mavar M, Reina MA, Puigdellívol-Sánchez A, San-Molina J, De Andrés JA (2014) Three-dimensional interactive model of lumbar spinal structures. Anaesthesia 69:521
33. Prats-Galino A, Reina MA, Mavar Haramija M, Juanes Méndez JA, De Andrés JA (2015) 3D interactive model of lumbar spinal structures of anesthetic interest. Clin Anat 28:205–212
34. Rhoton AL (2002) The supratentorial arteries. Neurosurgery 51: 53–120
35. Sorensen MS, Dobrzeniecki AB, Larsen P, Frisch T, Sporring J, Darvann TA (2002) The visible ear: a digital image library of the temporal bone. ORL J Otorhinolaryngol Relat Spec 64:378–381
36. Spiessberger A, Baumann F, Kothbauer KF, Aref M, Marbacher S, Fandino J, Nevzati E (2019) Bony dehiscence of the horizontal petrous internal carotid artery canal: an anatomic study with surgical implications. World Neurosurg:S1878–S8750
37. Sun X, Uan B, Truong HQ, Borghei-Razavi H, Snyderman CH, Fernández-Miranda JC (2018) A comparative analysis of endoscopic-assisted transoral and transnasal approaches to parapharyngeal space: a cadaveric study. J Neurol Surg B Skull Base 79:229–240
38. Tauber M, Van Loveren HR, Jallo G, Romano A, Keller JT (1999) The enigmatic foramen lacerum. Neurosurgery 44:386–391
39. Tubbs RS, Hansasuta A, Loukas M, Louis RG Jr, Shoja MM, Salter EG, Oakes WJ (2007) Branches of the petrous and cavernous segments of the internal carotid artery. Clin Anat 20:596–601
40. Üstün ME, Büyükmumcu M, Seker M, Karabulut AK, Uysal II, Ziylan T (2004) Possibility of middle meningeal artery-to-petrous internal carotid artery bypass: an anatomic study. Skull Base 14: 153–156
41. Valera-Melé M, Puigdellívol-Sánchez A, Mavar-Haramija M, Juanes-Méndez J, San-Román L, De Notaris M, Prats-Galino A (2018) A novel and freely available interactive 3D model of the internal carotid artery. J Med Sys 42:72
42. Van Loveren HR, Keller JT, El-Kalliny M, Scodary DJ, Tew JM (1991) The Dolenc technique for cavernous sinus exploration (cadaveric prosection). J Neurosurg 74:837–844
43. Vijaywarqiya M, Deopujari R, Athavale SA (2017) Anatomical study of petrous and cavernous parts of internal carotid artery. Anat Cell Biol 50:163–170
44. Wang S, Quin Y, Xiao D, Wu Z, Wei L (2018) Imaging evaluation of the location and fenestration of sellar floor during endonasal transsphenoidal surgery in patients with pituitary adenomas. World Neurosurg. https://doi.org/10.1016/j.wneu.2018.04.178
45. Wikimedia Commons. Gray H (1918) Anatomy of the Human Body, 20th ed. Philadelphia and New York:Lea&Febiger. (https://upload.wikimedia.org/wikipedia/commons/9/9c/Gray513.png). [Accessed June 1th, 2017]